

Rhodium-Mediated C–C Bond Activation of 2-(2',6'-Dialkylarylazo)-4-methylphenols. Elimination and Migration of Alkyl Groups

Suparna Bakshi,[†] Rama Acharyya,[†] Falguni Basuli,[†] Shie-Ming Peng,[‡] Gene-Hsiang Lee,[‡] Munirathinam Nethaji,[§] and Samaresh Bhattacharya^{*,†}

Department of Chemistry, Inorganic Chemistry Section, Jadavpur University, Kolkata 700 032, India,
Department of Chemistry, National Taiwan University, Taipei, Taiwan, Republic of China, and
Department of Inorganic and Physical Chemistry, Indian Institute of Science, Bangalore 560 012, India

Received August 13, 2007

Upon reaction of 2-(2',6'-dimethylphenylazo)-4-methylphenol with [Rh(PPh₃)₃Cl], the azo ligand undergoes an interesting rhodium-assisted C–C bond activation at one ortho position of the 2',6'-dimethylphenyl fragment, leading to the elimination of the methyl group from that ortho position. A similar elimination of an ethyl group takes place when 2-(2',6'-diethylphenylazo)-4-methylphenol is allowed to react with [Rh(PPh₃)₃Cl]. However, when 2-(2',6'-diisopropylphenylazo)-4-methylphenol reacts with [Rh(PPh₃)₃Cl], an interesting migration of an isopropyl group from its original location (say the 2' position) to the corresponding third position (say the 4' position) takes place. In all the three complexes the modified azo ligands bind to rhodium as dianionic C,N,O-donors, and two triphenylphosphines and a chloride are also coordinated to the metal center. Structures of all three complexes have been determined by X-ray crystallography. These complexes show characteristic ¹H NMR signals and intense MLCT transitions in the visible region. Cyclic voltammetry on these complexes shows a Rh(III)–Rh(IV) oxidation on the positive side of SCE and a reduction of the coordinated azo ligand on the negative side.

Introduction

There has been significant current interest in the utilization of transition metal complexes for bringing about interesting chemical transformations of organic substrates.¹ Such reactions often proceed via a C–H or C–C activation of the organic substrates,^{2,3} leading to the formation of reactive organometallic complexes, which finally yields the desired product, and hence synthesis of such organometallic species is of significant importance. The present work has emerged from our interest in the synthesis of organometallic complexes via platinum metal mediated C–H and C–C activation of some selected organic ligands, in general,⁴ and C–H activation of 2-(arylazo)-4-methylphenols (**I**) in particular.^{4e,h,i,k,m,o,r} It has been observed that upon reaction with different triphenylphosphine complexes of the platinum metals, these ligands (**I**) usually undergo C–H activation at one ortho position (say the 2' position) of the phenyl

ring in the arylazo fragment and bind to the metal center as tridentate C,N,O-donors (**II**), affording interesting cyclometalated complexes.^{4e,h,i,k,m,o,r} In the present study we have utilized three modified 2-(arylazo)phenols (**III**), viz., 2-(2',6'-dimethylphenylazo)-4-methylphenol (**L**¹), 2-(2',6'-diethylphenylazo)-4-methylphenol (**L**²), and 2-(2',6'-diisopropylphenylazo)-4-methylphenol (**L**³), in which both the ortho positions of the phenyl ring in the arylazo fragment are strategically blocked by three different alkyl groups. The main objective of this ligand modification was to see whether these modified ligands (**III**) undergo any C–C bond activation at the 2' position. In order to investigate the consequences of this ligand modification, rhodium has been selected as the platinum metal, and as a source of rhodium, the Wilkinson's catalyst, [Rh(PPh₃)₃Cl], has been utilized. Reactions of the three selected ligands (**L**¹, **L**², and **L**³) with [Rh(PPh₃)₃Cl] have indeed afforded three interesting organorhodium complexes via C–C bond activation at the 2' position of the azo ligands. The chemistry of these complexes

* Corresponding author. E-mail: samaresh_b@hotmail.com.

[†] Jadavpur University.

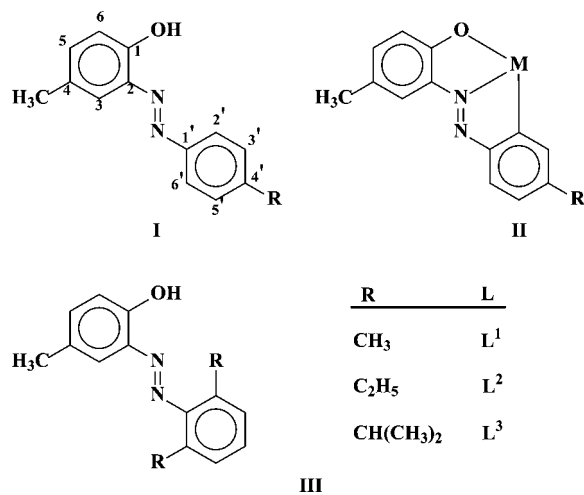
[‡] National Taiwan University.

[§] Indian Institute of Science.

(1) (a) Tsuji, J. *Transition Metal Reagents and Catalysts*; Wiley-VCH: Weinheim, 2000. (b) Hegedus, L. S. *Coord. Chem. Rev.* **1998**, *168*, 49. (c) Bellar, M.; Bolm, C., Eds. *Transition Metals for Organic Synthesis 1–2*; Wiley-VCH: Weinheim, 1998. (d) Cornils, B.; Hermann, W. A., Eds. *Applied Homogenous Catalysis with Organometallic Compounds: A Comprehensive Handbook in Two Volumes*; VCH: Weinheim, 1996. (e) Liebeskind, L. S., Ed. *Advances in Metal-Organic Chemistry*; Jai Press: Greenwich, CT, 1996. (f) Abel, E.; Stone, F. G. A.; Wilkinson, G., Eds. *Comprehensive Organometallic Chemistry*; Pergamon Press: Oxford, 1995, Vol. 12. (g) Hegedus, L. S. *Transition Metals in the Synthesis of Complex Organic Molecules*; Mill Valley, CA, 1994. (h) Collman, J. P.; Hegedus, L. S.; Norton, J. R.; Finke, R. G. *Principles and Applications of Organotransition Metal Chemistry*; Mill Valley, CA, 1987. (i) Trost, B. M.; Verhoeven, T. R. *Comprehensive Organometallic Chemistry*; Abel, E.; Stone, F. G. A.; Wilkinson, G., Eds.; Pergamon Press: Oxford, 1982; Vol. 8.

(2) (a) Jaeger-Fiedle, U.; Arndt, P.; Baumann, W.; Spannenberg, A.; Burlakov, V. V.; Rosenthal, U. *Eur. J. Inorg. Chem.* **2005**, *14*, 2842. (b) Keuseman, K. J.; Smolinkova, I. P.; Dunina, V. V. *Organometallics* **2005**, *24*, 4159. (c) Shi, L.; Tu, Y. Q.; Wang, M.; Zhao, F. M.; Fan, C. A.; Zhao, Y. M.; Xia, W. J. *J. Am. Chem. Soc.* **2005**, *127*, 10836. (d) Thalji, R. K.; Ahrendt, K. A.; Bergman, R. G.; Ellman, J. A. *J. Org. Chem.* **2005**, *70*, 6775. (e) Fan, Y.; Hall, M. B. *Organometallics* **2005**, *24*, 3827. (f) Driver, T. G.; Day, M. W.; Labinger, J. A.; Bercaw, J. E. *Organometallics* **2005**, *24*, 3644. (g) Esteruelas, M. A.; Lopez, A. M. *Organometallics* **2005**, *24*, 3584. (h) Rybtchinski, B.; Cohen, R.; Jan, M. L.; Milstein, D. *J. Am. Chem. Soc.* **2003**, *125*, 11041. (i) Pamplin, C. B.; Legzdins, P. *Acc. Chem. Res.* **2003**, *36*, 223. (j) Ritleng, V.; Sirlin, C.; Pfeffer, M. *Chem. Rev.* **2002**, *102*, 1731. (k) Rybtchinski, B.; Oevers, S.; Montag, M.; Vignalok, A.; Rozenberg, A.; Martin, J. M. L.; Milstein, D. *J. Am. Chem. Soc.* **2001**, *123*, 9064. (l) Vignalok, A.; Milstein, D. *Acc. Chem. Res.* **2001**, *34*, 798. (m) Slugovc, C.; Padilla-Martinez, I.; Sirol, S.; Carmona, E. *Coord. Chem. Rev.* **2001**, *213*, 129. (n) Jia, C.; Kitamura, T.; Fujiwara, Y. *Acc. Chem. Res.* **2001**, *34*, 633. (o) Sundermann, A.; Uzan, O.; Milstein, D.; Martin, J. M. L. *J. Am. Chem. Soc.* **2000**, *122*, 7095.

is reported herein, with special reference to their formation, structure, and spectroscopic and electrochemical properties.



Results and Discussion

As delineated in the Introduction, three 2-(2',6'-dialkylphenylazo)-4-methylphenols (**III**) have been utilized in the present study with the definite objective to see whether one of the two C–R bonds, at the 2' and 6' positions, undergoes C–C activation upon reaction with [Rh(PPh₃)₃Cl]. Reaction of the 2-(2',6'-dimethylphenylazo)-4-methylphenol (**L**¹) was first carried out with [Rh(PPh₃)₃Cl] in refluxing toluene in the presence of triethylamine, which afforded the blue complex **1**. Preliminary characterizations (microanalysis, mass, and ¹H NMR) on complex **1** hinted at the presence of two triphenylphosphines, a chloride, and a ligand **L**¹ and also indicated that ligand **L**¹ probably underwent some chemical transformation in the course of its binding to rhodium. For example, although ligand **L**¹ contains three methyl groups, the ¹H NMR spectrum of complex **1** showed two methyl signals of equal intensity at 1.82 and 2.33 ppm, indicating loss of a methyl group from the **L**¹ ligand during formation of complex **1**. The mass spectrum of this complex (Figure S1, Supporting Information) showed the [M + H]⁺ peak at 887, which is 15 units less than that expected for a rhodium complex containing two triphenylphosphines, a chloride, and a

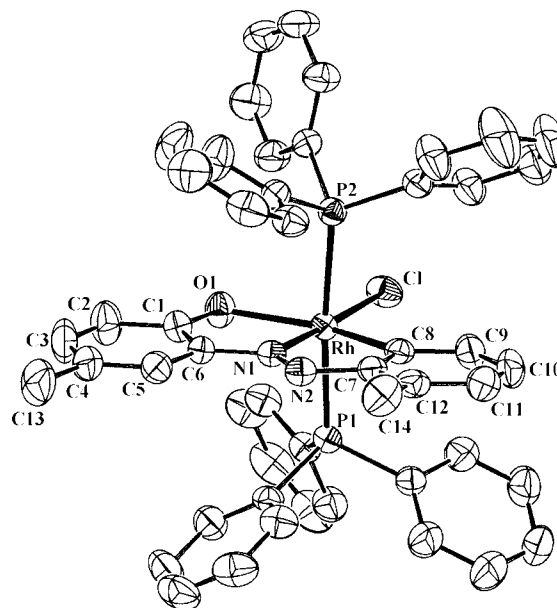


Figure 1. Structure of complex **1**.

deprotonated **L**¹, and thus the mass spectral data also supported loss of a methyl group from ligand **L**¹. Microanalytical data were also consistent with this speculated loss of a methyl group from ligand **L**¹. To verify this speculation, the identity of complex **1** was unveiled by its structure determination by X-ray crystallography. The structure is shown in Figure 1, and selected bond parameters are listed in Table 1. The structure shows that ligand **L**¹ has indeed undergone an interesting chemical transformation during the course of the synthetic reaction, in which one methyl group has been eliminated from one ortho position (say the 2' position) of the phenyl ring in the arylazo fragment and a direct metal–carbon bond has been established between the rhodium center and that particular phenyl ring carbon from which the methyl group has been lost. The modified **L**¹ ligand is thus coordinated to rhodium in a dianionic tridentate C,N,O-fashion (**IV**, R = CH₃). Two triphenylphosphines and a chloride are also bound to the metal center. Rhodium is therefore sitting in a CNOP₂Cl coordination environment, which is distorted octahedral in nature, as reflected in all the bond parameters around rhodium. The C,N,O-coordinated ligand and the chloride constitute one equatorial plane with the metal at

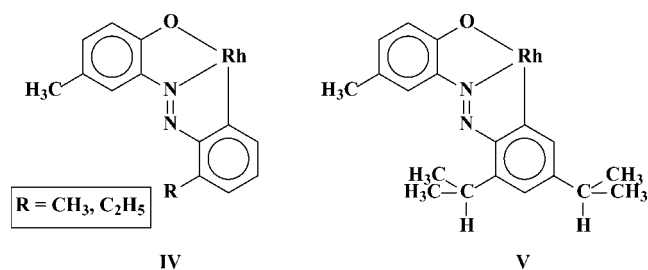
(3) (a) Albeniz, A. C.; Espinet, P.; Perez-Mateo, A.; Nova, A.; Ujaque, G. *Organometallics* **2006**, *25*, 1293. (b) Esteruelas, M. A.; Gonzalez, A. I.; Lopez, A. M.; Oliván, M.; Onate, E. *Organometallics* **2006**, *25*, 693. (c) Li, X.; Schopf, M.; Stephan, J.; Kipke, J.; Harms, K.; Sundermeyer, J. *Organometallics* **2006**, *25*, 528. (d) Ogo, S.; Takebe, Y.; Uehara, K.; Yamazaki, T.; Nakai, H.; Watanabe, Y.; Fukuzumi, S. *Organometallics* **2006**, *25*, 331. (e) Daquino, C.; Foti, M. C. *Tetrahedron* **2006**, *62*, 1536. (f) Schaefer, M.; Wolf, J.; Werner, H. *Dalton Trans.* **2005**, 1468. (g) Werner, H.; Muench, G.; Laubender, M. *Inorg. Chim. Acta* **2005**, *358*, 1510. (h) Tanaka, K.; Miyazawa, A.; Hiata, A.; Tashiro, M.; Saisyo, T.; Okabe, R.; Kohno, K.; Yamato, T. *J. Chem. Res.* **2005**, 495. (i) De Felice, Vincenzo; De Renzi, A.; Fraldi, N.; Roviello, G.; Tuzi, A. *J. Organomet. Chem.* **2005**, *690*, 2035. (j) Chin, C. S.; Lee, H.; Eum, M. S. *Organometallics* **2005**, *24*, 4849. (k) Cadierno, V.; Diez, J.; Garcia-Alvarez, J.; Gimeno, J. *Organometallics* **2005**, *24*, 2801. (l) Werner, H. *Organometallics* **2005**, *24*, 1036. (m) Maier, P.; Redlich, H.; Richter, J. *Tetrahedron: Asymmetry* **2005**, *16*, 3848. (n) Fleischer, H.; Schollmeyer, D. *Z. Naturforsch. B* **2005**, *60*, 1083. (o) Trifonov, A. A.; Fedorova, E. A.; Fukin, G. K.; Druzhkov, N. O.; Bochkarev, M. N. *Angew. Chem., Int. Ed.* **2004**, *43*, 5045. (p) Noveski, D.; Braun, T.; Neumann, B.; Stammler, A.; Stammler, H. G. *Dalton Trans.* **2004**, 4106. (q) Schmid, R.; Kirchner, K. *Eur. J. Inorg. Chem.* **2004**, 2609. (r) Li, X.; Appelhans, L. N.; Fallner, J. W.; Crabtree, R. H. *Organometallics* **2004**, *23*, 3378. (s) Navarro, J.; Sola, E.; Martin, M.; Dobrinovitch, I. T.; Lahoz, F. J.; Oro, L. A. *Organometallics* **2004**, *23*, 1908. (t) Werner, H.; Mahr, N.; Schneider, M. E.; Bosch, M.; Wolf, J. *Polyhedron* **2004**, *23*, 2645. (u) Zippel, T.; Arndt, P.; Ohff, A.; Spannenberg, A.; Kempe, R.; Rosenthal, U. *Organometallics* **1998**, *17*, 4429.

(4) (a) GuhaRoy, C.; Sen, S. S.; Dutta, S.; Mostafa, G.; Bhattacharya, S. *Polyhedron* **2007**, *26*, 3876. (b) Nag, S.; Butcher, R. J.; Bhattacharya, S. *Eur. J. Inorg. Chem.* **2007**, 1251. (c) Baksi, S.; Acharyya, R.; Dutta, S.; Blake, A. J.; Drew, M. G. B.; Bhattacharya, S. *J. Organomet. Chem.* **2007**, *692*, 1025. (d) Halder, S.; Drew, M. G. B.; Bhattacharya, S. *Organometallics* **2006**, *25*, 5969. (e) Halder, S.; Acharyya, R.; Peng, S. M.; Lee, G. H.; Drew, M. G. B.; Bhattacharya, S. *Inorg. Chem.* **2006**, *45*, 9654. (f) Basu, S.; Dutta, S.; Drew, M. G. B.; Bhattacharya, S. *J. Organomet. Chem.* **2006**, *691*, 3581. (g) Acharyya, R.; Dutta, S.; Basuli, F.; Peng, S. M.; Lee, G. H.; Falvello, L. R.; Bhattacharya, S. *Inorg. Chem.* **2006**, *45*, 1252. (h) Gupta, P.; Dutta, S.; Basuli, F.; Peng, S. M.; Lee, G. H.; Bhattacharya, S. *Inorg. Chem.* **2006**, *45*, 460. (i) Acharyya, R.; Basuli, F.; Peng, S. M.; Lee, G. H.; Wang, R. Z.; Mak, T. C. W.; Bhattacharya, S. *J. Organomet. Chem.* **2005**, *690*, 3908. (j) Nag, S.; Gupta, P.; Butcher, R. J.; Bhattacharya, S. *Inorg. Chem.* **2004**, *43*, 4814. (k) Acharyya, R.; Basuli, F.; Wang, R. Z.; Mak, T. C. W.; Bhattacharya, S. *Inorg. Chem.* **2004**, *43*, 704. (l) Acharyya, R.; Peng, S. M.; Lee, G. H.; Bhattacharya, S. *Inorg. Chem.* **2003**, *42*, 7378. (m) Gupta, P.; Butcher, R. J.; Bhattacharya, S. *Inorg. Chem.* **2003**, *42*, 5405. (n) Pal, I.; Dutta, S.; Basuli, F.; Goverdhan, S.; Peng, S. M.; Lee, G. H.; Bhattacharya, S. *Inorg. Chem.* **2003**, *42*, 4338. (o) Majumder, K.; Peng, S. M.; Bhattacharya, S. *J. Chem. Soc., Dalton Trans.* **2001**, 284. (p) Das, A.; Basuli, F.; Falvello, L. R.; Bhattacharya, S. *Inorg. Chem.* **2001**, *40*, 4085. (q) Basuli, F.; Peng, S. M.; Bhattacharya, S. *Inorg. Chem.* **2001**, *40*, 1126. (r) Dutta, S.; Peng, S. M.; Bhattacharya, S. *J. Chem. Soc., Dalton Trans.* **2000**, 4623.

Table 1. Selected Bond Distances and Bond Angles for Complexes 1, 2, and 3

Complex 1			
Bond Distances (Å)			
Rh–C11	2.3786(12)	Rh–N1	1.953(3)
Rh–P1	2.3565(9)	Rh–C8	1.998(4)
Rh–P2	2.3727(9)	C1–O1	1.303(5)
Rh–O1	2.194(3)	N1–N2	1.279(4)
Bond Angles (deg)			
P1–Rh–P2	174.19(4)	O1–Rh–N1	80.28(11)
C11–Rh–N1	178.22(9)	N1–Rh–C8	79.11(14)
O1–Rh–C8	159.38(14)		
Complex 2			
Bond Distances (Å)			
Rh–C11	2.367(3)	Rh–N1	1.941(9)
Rh–P1	2.357(3)	Rh–C15	1.998(11)
Rh–P2	2.355(3)	C1–O1	1.294(15)
Rh–O1	2.179(7)	N1–N2	1.253(13)
Bond Angles (deg)			
P1–Rh–P2	174.07(10)	O1–Rh–N1	80.8(3)
C11–Rh–N1	178.0(2)	N1–Rh–C15	78.4(4)
O1–Rh–C15	159.2(4)		
Complex 3			
Bond Distances (Å)			
Rh–C11	2.379(2)	Rh–N1	1.957(7)
Rh–P1	2.363(2)	Rh–C19	2.000(8)
Rh–P2	2.357(2)	C1–O1	1.292(12)
Rh–O1	2.180(5)	N1–N2	1.280(10)
Bond Angles (deg)			
P1–Rh–P2	172.51(7)	O1–Rh–N1	80.1(3)
C11–Rh–N1	177.3(2)	N1–Rh–C19	78.9(3)
O1–Rh–C19	159.0(3)		

the center, while the two PPh₃ ligands occupy the remaining two axial positions, and hence they are mutually *trans*. The Rh–C, Rh–N, Rh–O, Rh–P, and Rh–Cl distances are all quite normal, as usually observed in complexes of rhodium(III) containing these bonds.^{4r}



The absence of any solvent of crystallization in the crystal lattice of complex 1 indicates the possible existence of noncovalent interactions between the individual complex molecules. To sort this out, the packing pattern in the lattice has been examined, which shows that a hydrogen-bonding interaction of a single type, viz., C–H... π interaction, is active in the lattice (Figure 2). One methyl C–H in the arylazo fragment of each complex molecule is hydrogen-bonded to the π -cloud over a phenyl ring of a PPh₃ ligand belonging to an adjacent complex molecule. In addition, phenyl C–H's of different PPh₃ ligands are found to be involved in intermolecular hydrogen-bonding interactions with the π -cloud over phenyl rings of PPh₃ ligands as well as of the azo ligand. Through such C–H... π interactions each complex molecule is linked to six neighboring molecules, and these hydrogen-bonding interactions are extended throughout the entire lattice; they appear to be responsible for holding the crystal together. It may be mentioned in this context that

such hydrogen-bonding interactions are of significant current interest in crystal engineering as well as in biology.⁵

Elimination of a methyl group from ligand L¹ upon its reaction with [Rh(PPh₃)₃Cl] via rhodium-assisted C–C bond activation has prompted us to explore similar reactions with other 2-(2',6'-dalkylphenylazo)-4-methylphenols. Hence the other two related ligands, viz., 2-(2',6'-diethylphenylazo)-4-methylphenol (L²) and 2-(2',6'-diisopropylphenylazo)-4-methylphenol (L³), were tried. Reactions of these two ligands with [Rh(PPh₃)₃Cl] were carried out under experimental conditions similar to those used before, and two new rhodium complexes, 2 and 3, were obtained. As observed in the case of complex 1, preliminary characterizations on complex 2 again indicated that two triphenylphosphines, a chloride, and a monodeethylated L² ligand are coordinated to rhodium. The loss of an ethyl fragment from L² was indicated by both the ¹H NMR spectrum of complex 2, showing a signal for only one ethyl group, and its mass spectrum (Figure S2, Supporting Information), showing the [M + H]⁺ peak at 901, which is 29 units less than that expected for a rhodium complex containing two triphenylphosphines, a chloride, and a deprotonated L². The observed microanalytical data also supported this loss of an ethyl group from L². For an unambiguous characterization of complex 2 as well as to authenticate the status of ligand L² in it, its structure was determined by X-ray crystallography. The structure (Figure 3) shows that one ethyl fragment has indeed been lost from ligand L² during formation of complex 2, and the modified ligand is bound to rhodium as a C,N,O-donor (IV, R = C₂H₅). Two triphenylphosphines, which are mutually *trans*, and a chloride are also coordinated to the metal center. The structural parameters of complex 2 are similar to those of complex 1 (Table 1). An examination of the packing pattern in the lattice of complex 2 shows that C–H... π interactions, involving different phenyl C–H's of the PPh₃ ligands and π -cloud over the phenyl rings of both PPh₃ and the azo-ligand, are active in the lattice (Figure S3, Supporting Information).

Preliminary characterization of complex 3 indicated the presence of two triphenylphosphines, a chloride, and a ligand L³. However, unlike complexes 1 and 2, no indication of loss of any isopropyl group from ligand L³ during formation of complex 3 was obtained. For example, the ¹H NMR spectrum of complex 3 shows clear signals for two isopropyl groups. At the same time, the NMR spectrum also shows three singlets (1H each) in the aromatic region at 5.85, 6.44, and 6.93 ppm, and as only one such singlet could be expected from the para-cresol fragment of the azo-ligand, the appearance of these three singlets was rather surprising. The mass spectrum of complex 3 (Figure S4, Supporting Information) shows the [M + H]⁺ peak at 957, as expected for a rhodium complex containing two

(5) (a) Burley, S. K.; Petsko, G. A. *Science* **1985**, 229, 23. (b) Weiss, H. C.; Blaser, D.; Boese, R.; Doughan, B. M.; Haley, M. M. *Chem. Commun.* **1997**, 1703. (c) Madhavi, N. N. L.; Katz, A. K.; Carrell, H. L.; Nangia, A.; Desiraju, G. R. *Chem. Commun.* **1997**, 1953. (d) Burley, S. K.; Petsko, G. A. *Adv. Protein Chem.* **1988**, 39, 125. (e) Nishio, M.; Hirota, M.; Umezawa, Y. *The CH... π Interactions (Evidence, Nature and Consequences)*; Wiley-VCH: New York, 1998. (f) Umezawa, Y.; Tsuboyama, S.; Honda, K.; Uzawa, J.; Nishio, M. *Bull. Chem. Soc. Jpn.* **1998**, 71, 120. (g) Desiraju, G. R.; Steiner, T. *The Weak Hydrogen Bond (IUCr Monograph on Crystallography 9)*; Oxford Science Pub., 1999. (h) Hannon, M. J.; Painting, C. L.; Alcock, N. W. *Chem. Commun.* **1999**, 2023. (i) Mcnelis, B. J.; Nathan, L. C.; Clark, C. J. *J. Chem. Soc., Dalton Trans.* **1999**, 1831. (j) Biradha, K.; Seward, C.; Zaworotko, M. J. *Angew. Chem., Int. Ed.* **1999**, 38, 492. (k) Calhorda, M. J. *Chem. Commun.* **2000**, 801. (l) Janiak, C.; Temizdemir, S.; Dechert, S. *Inorg. Chem. Commun.* **2000**, 3, 271. (m) Janiak, C.; Temizdemir, S.; Dechert, S.; Deck, W.; Girgsdies, F.; Heinze, J.; Kolm, M. J.; Scarmann, T. G.; Zipffel, O. M. *Eur. J. Inorg. Chem.* **2000**, 1229.

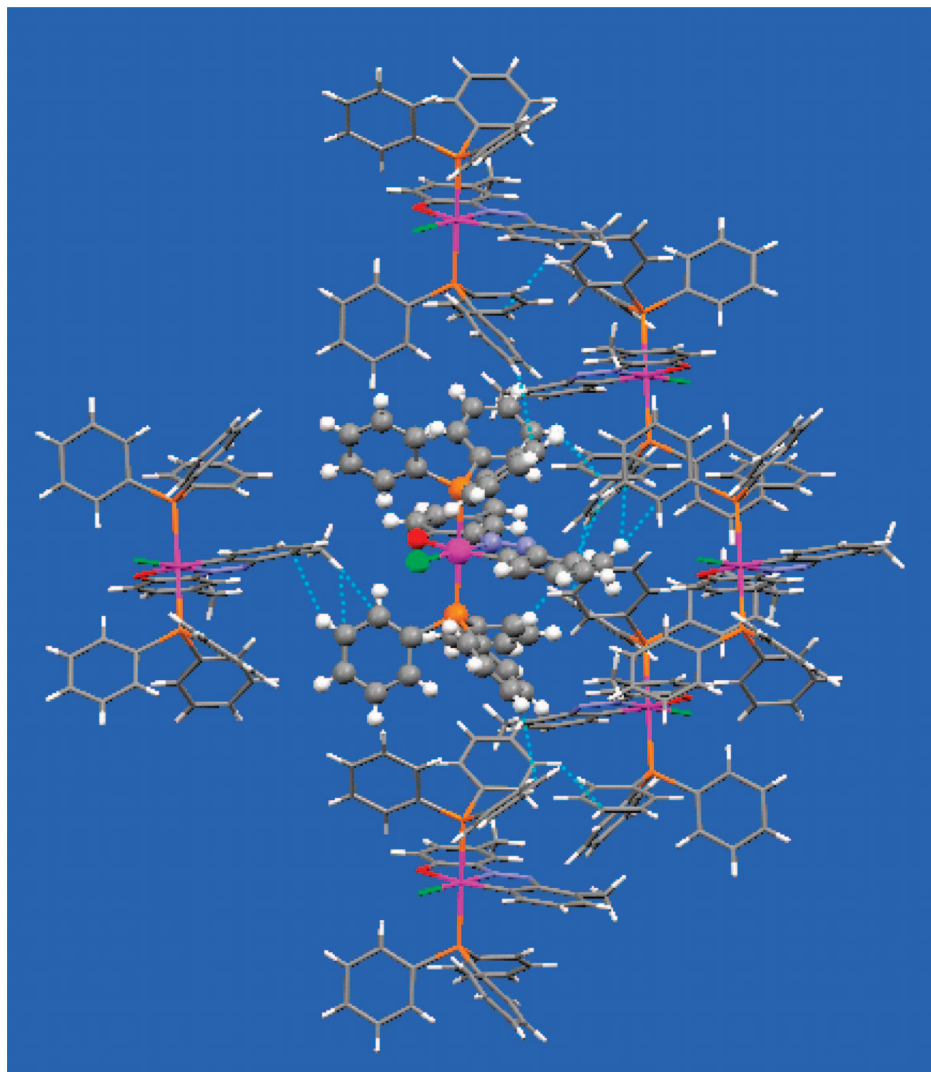


Figure 2. C–H... π interactions in complex **1**.

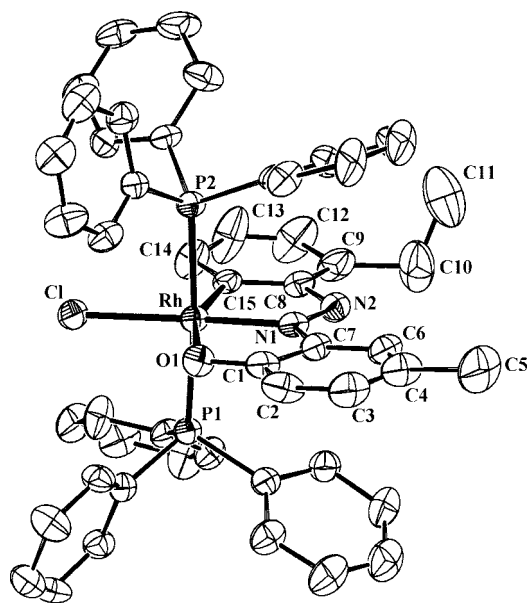


Figure 3. Structure of complex **2**.

triphenylphosphines, a chloride, and a deprotonated L^3 . The observed microanalytical data were also in accordance with this formulation. For an unambiguous characterization of complex

3 as well as to ascertain the status of ligand L^3 in it, its structure has also been determined by X-ray crystallography. The structure (Figure 4) reveals that an interesting transformation of ligand L^3 has taken place during formation of complex **3**, whereby one isopropyl group has migrated from its original location (say the 2' position) and is inserted (via loss of a proton) into the C–H bond at the corresponding 4' position, thus generating an isopropyl group at the 4' position, and the modified ligand is bound to rhodium as a C,N,O-donor (**V**). The other structural features of complex **3** are similar to those of complexes **1** and **2** (Table 2). An examination of the packing pattern in the lattice of complex **3** shows that intermolecular C–H... π interactions, similar to those observed in complex **2**, have linked the different molecules in the lattice and thus have given it the observed stability (Figure S5, Supporting Information).

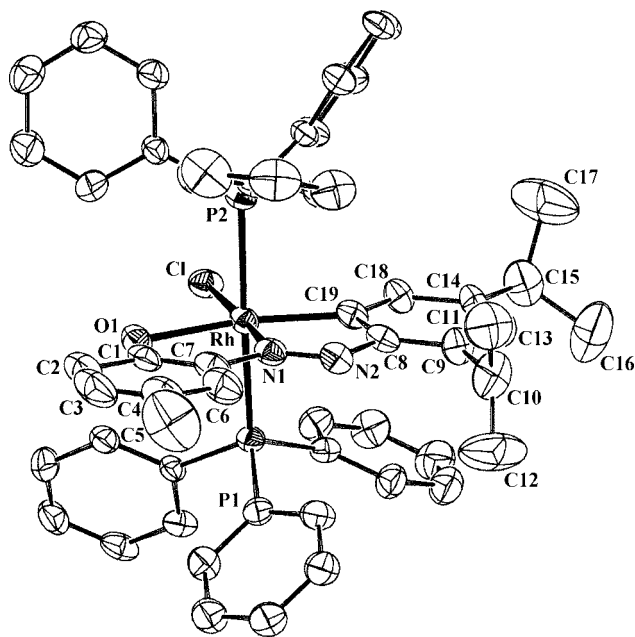
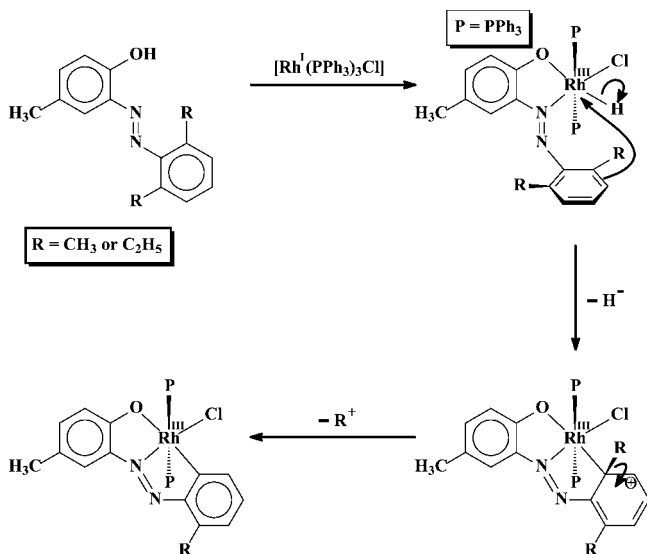
The exact mechanisms behind the observed transformations of ligand L^1 , L^2 , and L^3 during formation of complexes **1**, **2**, and **3**, respectively, are not completely clear to us. However, some speculated sequences shown in Scheme 1 and Scheme 2 seem probable.

During reaction of ligand L^1 or L^2 with the rhodium(I) center of $[\text{Rh}(\text{PPh}_3)_3\text{Cl}]$, the phenolic O–H bond of the azo-ligand seems to undergo rhodium-assisted activation in the initial step, whereby it oxidatively binds to the metal center, generating a hydride complex of rhodium(III) as the reactive intermediate

Table 2. Electronic Spectral and Cyclic Voltammetric Data

compound	electronic spectral data ^a λ_{\max} , nm (ϵ , M ⁻¹ cm ⁻¹)	cyclic voltammetric data ^{a,b}
1	630(11200), 592(9800), 384 ^c (10500), 339 ^c (18700), 289(62300)	0.79 ^d (90) ^e , -1.05 ^f
2	626(11700), 585 ^c (10600), 386 ^c (10900), 333 ^c (19100), 290(43000)	0.97 ^d (270) ^e , -0.99 ^f
3	624(10200), 588 ^c (10300), 382 ^c (12101), 342 ^c (15923), 289(32484)	1.03 ^d (327) ^e , -1.25 ^f

^a In acetonitrile. ^b Supporting electrolyte, TBAP; scan rate 50 mV s⁻¹; reference electrode, SCE. ^c Shoulder. ^d $E_{1/2} = 0.5(E_{pa} + E_{pc})$, where E_{pa} and E_{pc} are anodic and cathodic peak potentials, respectively. ^e $\Delta E_p = (E_{pa} - E_{pc})$. ^f E_{pc} value.

**Figure 4.** Structure of complex **3**.**Scheme 1. Probable Steps in the Formation of Complexes 1 and 2**

(Scheme 1). This is followed by formation of a metal–carbon bond from one ortho position (say the 2' position) of the phenyl ring in the phenylazo fragment, causing loss of aromaticity of that ring and generating a positive charge at the 3' position. Formation of the rhodium–carbon bond is associated with simultaneous dissociation of the coordinated hydride, which probably triggers loss of the R group from the 2' position as a carbocation, and thus the lost aromaticity of the phenyl ring is regained, affording the organorhodium complexes **1** and **2**. Considering the last two steps together, formation of complexes **1** and **2** from the hydride intermediate occurs via loss of RH

(methane in the case of **1** and ethane in the case of **2**). Upon reaction of ligand **L**³ with [Rh(PPh₃)₃Cl], a similar hydride intermediate is formed in the first step (Scheme 2), which is followed, as before, by formation of a metal–carbon bond with simultaneous loss of the hydride. In the next step, unlike loss of the alkyl group as seen before, loss of the central proton from the isopropyl group at the 2' position seems to be happening. Subsequently a C–C bond is formed between the central carbon of the deprotonated isopropyl group and the ring carbon at the 3' position having the positive charge. This is followed by migration of the C(CH₃)₂ fragment, which was bound in an η^2 -fashion to the 2',3' ring carbons, to the corresponding 3',4' position. In the next step usual rearrangements in the η^2 -bound C(CH₃)₂ fragment take place, affording complex **3**. Formation of complex **3**, from the hydride intermediate, thus occurs via loss of molecular hydrogen.

Magnetic susceptibility measurements showed that all the complexes are diamagnetic, which corresponds to the +3 oxidation state of rhodium (low-spin d⁶, $S = 0$) in these complexes. ¹H NMR spectra of the complexes have been recorded in CDCl₃ solution. Each complex shows broad signals within 7.0–7.7 ppm for the coordinated PPh₃ ligands. The methyl signal from the phenol fragment is observed as a distinct peak near 1.8 ppm. The other aliphatic proton signals originating from the methyl, ethyl, and isopropyl groups of the coordinated ligands appear at their usual positions. Among the expected aromatic proton signals for the coordinated azo-ligands, most have been clearly observed, while a few could not be detected due to their overlap with the PPh₃ signals. Infrared spectra of the complexes show sharp bands near 746, 696, and 518 cm⁻¹, due to the coordinated PPh₃ ligands. Strong bands are also observed near 1483, 1434, 1380, 1305, 1244, 1190, and 1093 cm⁻¹ in all these complexes, which are absent in the infrared spectrum of [Rh(PPh₃)₃Cl], and hence these bands are attributed to the coordinated azo-ligands. The ¹H NMR and IR spectral data of the complexes are therefore consistent with their compositions.

The complexes **1**, **2**, and **3** are found to be soluble in dichloromethane, chloroform, acetonitrile, acetone, etc., producing intense blue solutions. Electronic spectra of these complexes have been recorded in acetonitrile solution. Each complex shows several intense absorptions in the ultraviolet and visible region (Table 2). The absorptions in the ultraviolet region are assignable to transitions within the ligand orbitals. To understand the origin of the absorptions in the visible region, EHMO calculations have been performed on computer-generated models of all the three complexes,⁶ where phenyl rings of the PPh₃ ligands have been replaced by hydrogens. Compositions of selected molecular orbitals are given in Table 3, and the partial MO diagram of complex **1** is shown in Figure 5. Partial MO diagrams of complexes **2** and **3** are deposited as Figure S6 and Figure S7 (Supporting Information). The calculations show that the highest occupied molecular orbital (HOMO) has major (>74%) contribution from the metal d-orbitals, whereas the lowest unoc-

(6) (a) Mealli, C.; Proserpio, D. M. *CACAO Version 4.0*; Italy, 1994. (b) Mealli, C.; Proserpio, D. M. *J. Chem. Educ.* **1990**, *67*, 399.

Scheme 2. Probable Steps in the Formation of Complex 3

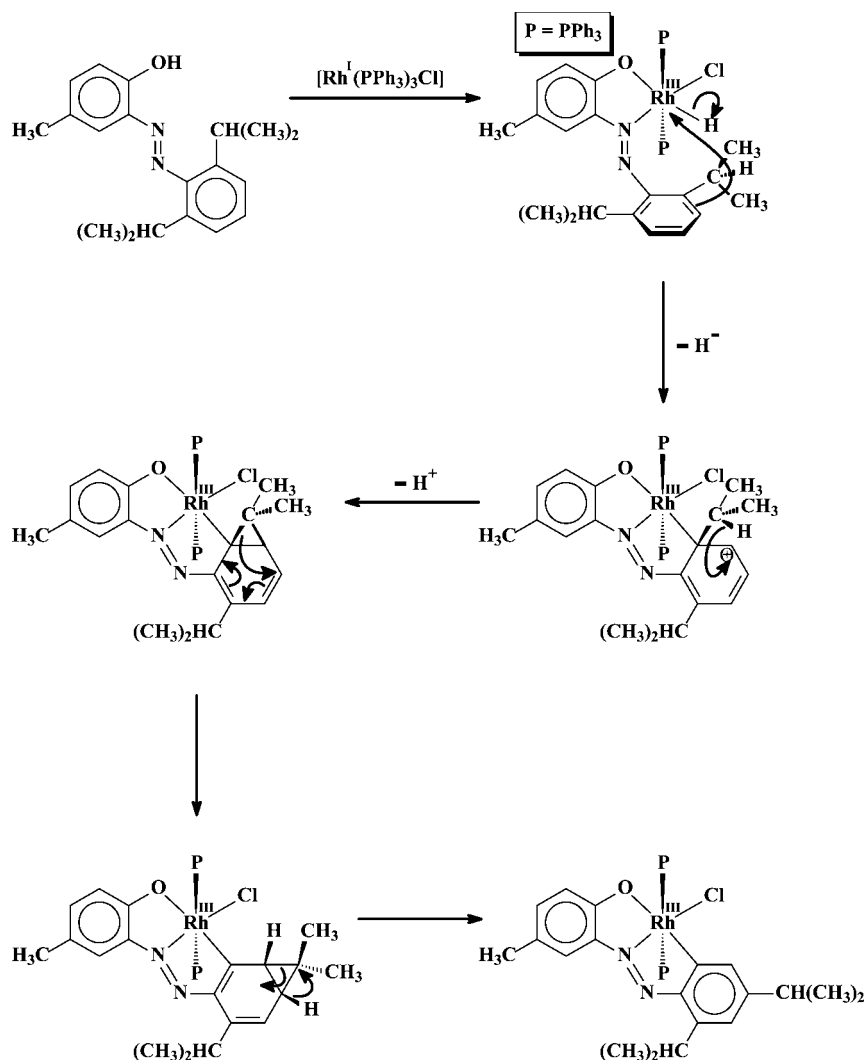


Table 3. Composition of Selected Molecular Orbitals

compound	contributing fragments	% contribution of fragments to					
		HOMO	HOMO–1	HOMO–2	LUMO	LUMO+1	LUMO +2
1	Rh	78	41	57	13	2	
	Cl	5		5			
	ONCligand	9	55	32	84 (N=N,50)	91	91
2	Rh	75	49	44	21	2	
	Cl	13	17		2		
	ONCligand	6	24	52	75 (N=N,46)	89	92
3	Rh	74	16	34	12		2
	Cl	4					
	ONCligand	10	68	38	81 (N=N,50)	97	91

occupied molecular orbital (LUMO) is primarily (>75%) delocalized over the coordinated C,N,O-donor ligand and is concentrated heavily (>46%) on the azo fragment. Hence the lowest energy absorption in the visible region is assignable to a charge-transfer transition from the filled rhodium orbital (HOMO) to the π^* (azo)-orbital (LUMO) of the tridentate ligand. The other absorptions in the visible region are attributable to transitions occurring from the other filled orbitals to the higher energy vacant orbitals.

Electrochemical properties of the complexes have been studied by cyclic voltammetry in acetonitrile solution (0.1 M TBAP). Each complex shows one oxidative response on the positive side of the SCE and one reductive response on the negative side (Table 2). A selected voltammogram is shown in

Figure 6. Keeping the composition of the HOMO in view, the oxidation is assigned to Rh(III)–Rh(IV) oxidation. Similarly in view of composition of the LUMO, the reduction is attributed to reduction of the azo group of the C,N,O-coordinated ligand. The oxidative responses are quasi-reversible in nature, while the reductive responses are completely irreversible, which indicates that the oxidized species has little stability but the reduced species is totally unstable in nature and undergoes rapid decomposition. One-electron stoichiometry of both the redox responses has been established by comparing their current heights (i_{pa} for oxidative response and i_{pc} for reductive response) with those of the standard ferrocene–ferrocenium couple under identical experimental conditions.

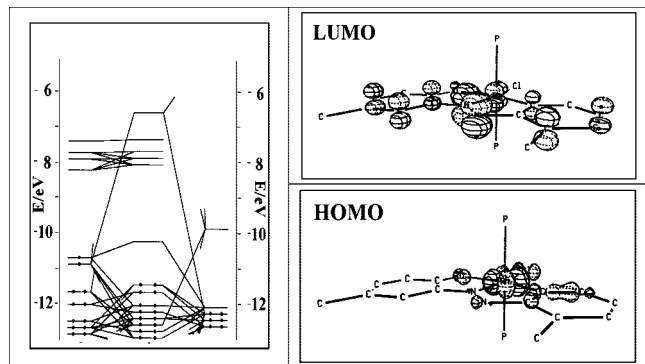


Figure 5. Partial molecular orbital diagram of complex 1.

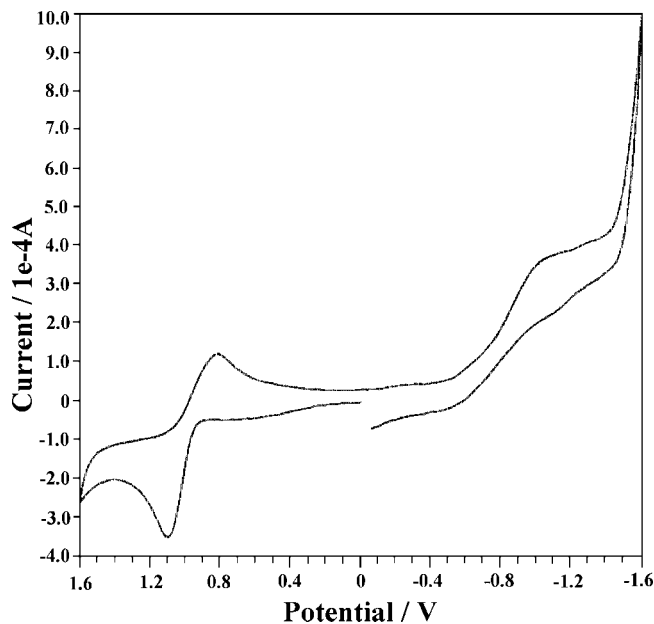


Figure 6. Cyclic voltammogram of complex 2 in acetonitrile solution (0.1 M TBAP) at a scan rate of 50 mV s⁻¹.

Conclusion

The present study shows that blocking both the 2',6' positions of the 2-(arylo)phenol (**I**) by alkyl groups can successfully induce metal-mediated C–C bond activation at one of these two positions, which has been manifested by reaction of the 2-(2',6'-dialkylphenylazo)-4-methylphenols (**III**) with [Rh(PPh₃)₃Cl]. Each of the three selected azo ligands (**L**¹, **L**², and **L**³) is found to undergo interesting chemical transformation, viz., loss or migration of an alkyl group from the 2' position, and this study also demonstrated that the nature of the transformation of the azo ligand is dependent on the nature of the alkyl group at the 2',6' positions.

Experimental Procedures

Materials. Rhodium trichloride was purchased from Arora Matthey, Kolkata, India. 2,6-Dimethylaniline, 2,6-diethylaniline, and 2,6-diisopropylaniline were obtained from Loba Chemie, Mumbai, India. Triphenylphosphine and *p*-cresol were purchased from S. D. Fine-Chem Limited, Mumbai, India. [Rh(PPh₃)₃Cl] was prepared by following a reported procedure.⁷ Preparation of tetrabutylammonium perchlorate (TBAP) for electrochemical work was per-

formed as reported in the literature.⁸ All other chemicals and solvents were reagent-grade commercial materials and were used as received.

Preparation of Compounds. **L**¹. 2',6'-Dimethylaniline (5 g, 0.04 mol) was dissolved in 1:1 HCl (30 mL). The solution was diazotized with NaNO₂ (2.8 g, 0.04 mol) in water (20 mL) at 0 °C. Separately *p*-cresol (4.5 g, 0.04 mol) was dissolved in 10% NaOH solution (30 mL) and the solution was cooled to 0 °C. The diazotized solution was then added slowly to the alkaline solution of *p*-cresol with continuous stirring in an ice-bath (0 °C). Then it was acidified with 1:1 HCl. Stirring was continued for 30 min. The red precipitate was collected by filtration, thoroughly washed with water, and dried in vacuo over P₄O₁₀. Purification was achieved by thin-layer chromatography on a silica plate with hexane as the eluant. A red band separated, which was extracted with hexane. Upon slow evaporation of the extract, 2-(2',6'-dimethylphenylazo)-4-methylphenol (**L**¹) was obtained as a red solid. Yield: 70%. Anal. Calcd for C₁₅H₁₆N₂O: C, 75.00; H, 6.66; N, 11.66. Found: C, 75.15; H, 6.54; N, 11.67. ¹H NMR:⁹ 2.43 (s, 6H); 2.47 (s, 3H); 6.95 (d, 1H, *J* = 8.5); 7.13–7.26* (4H); 7.75 (s, 1H); 12.71 (s, OH).

L². This was prepared by following the same above procedure using 2',6'-diethylaniline instead of 2',6'-dimethylaniline. Instead of a red precipitate (as observed for **L**¹), an orange oily layer separated, which was extracted with hexane. The hexane extract was evaporated to yield an orange oily liquid, which was purified by thin-layer chromatography on a silica plate with hexane as the eluant. An orange band separated, which was extracted with hexane. Upon slow evaporation of the extract, 2-(2',6'-diethylphenylazo)-4-methylphenol (**L**²) was obtained as a thick orange liquid. Yield: 60%. Anal. Calcd for C₁₇H₂₀N₂O: C, 76.12; H, 7.46; N, 10.45. Found: C, 76.35; H, 7.43; N, 10.44. ¹H NMR: 1.23 (t, 6H, *J* = 7.8); 2.40 (s, 3H); 2.71 (q, 4H, *J* = 7.4); 6.96 (d, 1H, *J* = 8.3); 7.17–7.28*(4H); 7.74 (s, 1H); 12.60 (s, OH).

L³. This was obtained as an orange liquid by following the same above procedure (as in **L**²) using 2',6'-diisopropylaniline instead of 2',6'-diethylaniline. Yield: 65%. Anal. Calcd for C₁₉H₂₄N₂O: C, 77.03; H, 8.11; N, 9.46. Found: C, 77.15; H, 8.16; N, 9.51. ¹H NMR: 1.27 (d, 12H, *J* = 6.7); 2.44 (s, 3H); 3.11 (m*, 2H, 7.02–7.40*(5H); 7.82 (s, 1H); 12.54 (s, OH).

1. To a solution of **L**¹ (26 mg, 0.11 mmol) in toluene (40 mL) was added [Rh(PPh₃)₃Cl] (100 mg, 0.11 mmol) followed by triethylamine (11 mg, 0.11 mmol). The resulting mixture was then heated at reflux for 24 h to yield a dark red solution. The solvent was then evaporated to give a solid mass, which was subjected to purification by thin-layer chromatography on a silica plate. With benzene as the eluant, a blue band separated, which was extracted with acetonitrile. Evaporation of this extract gave complex **1** as a dark crystalline solid. Yield: 35%. Anal. Calcd for C₅₀H₄₂N₂O₂ClRh: C, 67.76; H, 4.74; N, 3.16. Found: C, 67.35; H, 4.76; N, 3.14. ¹H NMR: 1.82 (s, 3H); 2.33 (s, 3H); 5.88 (s, 1H); 6.25 (d, 1H, *J* = 8.7); 6.34 (t, 1H, *J* = 7.6); 6.50 (d, 2H, *J* = 6.9); 7.08–7.55* (2PPh₃).

The other two complexes (**2** and **3**) were prepared by following the same above procedure using ligand **L**² and **L**³, respectively, instead of **L**¹.

2. Yield: 28%. Anal. Calcd for C₅₁H₄₄N₂O₂ClRh: C, 68.04; H, 4.89; N, 3.11. Found: C, 68.35; H, 4.86; N, 3.13. ¹H NMR: 1.83 (s, 3H); 2.75 (q, 2H, *J* = 7.5); 5.90 (s, 1H); 6.28 (d, 1H, *J* = 7.9); 6.39 (t, 1H, *J* = 7.5); 6.56 (d, 2H, *J* = 7.9); 7.08 (d, 1H, *J* = 7.8); 7.14–7.72* (2PPh₃). **3.** Yield: 25%. Anal. Calcd for C₅₅H₅₂N₂O₂ClRh: C, 69.07; H, 5.55; N, 2.93. Found: C, 68.89;

(8) (a) Sawyer, D. T.; Roberts, J. L., Jr. *Experimental Electrochemistry for Chemists*; Wiley: New York, 1974; pp 167–215. (b) Walter, M.; Ramaley, L. *Anal. Chem.* **1973**, *45*, 165.

(9) Chemical shifts are given in ppm, and multiplicity of the signals along with the associated coupling constants (*J* in Hz) are given in parentheses. Overlapping signals are marked with an asterisk.

(7) Osborn, J. A.; Wilkinson, G. *Inorg. Synth.* **1967**, *10*, 67.

Table 4. Crystallographic Data for Complexes 1, 2, and 3

	1	2	3
empirical formula	C ₅₀ H ₄₂ ClN ₂ OP ₂ Rh	C ₅₁ H ₄₄ N ₂ ClOP ₂ Rh	C ₅₅ H ₅₂ ClN ₂ OP ₂ Rh
fw	887.16	901.18	957.29
space group	monoclinic, <i>P</i> ₂ ₁ / <i>c</i>	monoclinic, <i>P</i> ₂ ₁ / <i>n</i>	monoclinic, <i>P</i> ₂ ₁ / <i>c</i>
<i>a</i> (Å)	18.1980 (7)	18.463 (10)	15.887 (5)
<i>b</i> (Å)	11.9925 (5)	12.007 (7)	12.016 (4)
<i>c</i> (Å)	20.5405 (8)	20.898 (12)	25.410 (9)
β (deg)	112.5470 (10)	92.519 (10)	100.139 (7)
<i>V</i> (Å ³)	4140.1 (3)	4628 (5)	4775 (3)
<i>Z</i>	4	4	4
λ (Å)	0.71073	0.71073	0.71073
cryst size (mm ³)	0.12 × 0.15 × 0.20	0.03 × 0.11 × 0.34	0.16 × 0.22 × 0.65
<i>T</i> (K)	295	293	293
μ (mm ⁻¹)	0.595	0.534	0.521
R1 ^a	0.0565	0.1199	0.0750
wR2 ^b	0.1282	0.3744	0.2113
GOF ^c	1.18	0.98	0.88

^a $R1 = \sum ||F_o| - |F_c|| / \sum |F_o|$, ^b $wR2 = [\sum \{w(F_o^2 - F_c^2)^2\} / \sum \{w(F_o^2)\}]^{1/2}$, ^c $GOF = [\sum (w(F_o^2 - F_c^2)^2) / (M - N)]^{1/2}$, where *M* is the number of reflections and *N* is the number of parameters refined.

H, 5.46; N, 3.03. ¹H NMR: 0.918 (d, 6H, *J* = 6.9); 1.81 (s, 3H); 5.85 (s, 3H); 6.26 (d, 1H, *J* = 8.8); 6.93 (s, 1H); 7.11–7.68 (2PPh₃).

Physical Measurements. Microanalyses (C, H, N) were done using a Heraeus Carlo Erba 1108 elemental analyzer. Magnetic susceptibilities were measured using a PAR 155 vibrating sample magnetometer fitted with a Walker Scientific L75FBAL magnet. Mass spectra were recorded with a Micromass LCT electrospray (Qtof Micro YA263) mass spectrometer by electrospray ionization method. IR spectra were obtained on a Shimadzu FTIR-8300 spectrometer with samples prepared as KBr pellets. ¹H NMR spectra in CDCl₃ solutions were obtained on a Bruker Avance DPX 300 NMR spectrometer using TMS as the internal standard. Electronic spectra were recorded on a JASCO V-570 spectrophotometer. Electrochemical measurements were made using a CH Instruments model 600A electrochemical analyzer. A platinum disk working electrode, a platinum wire auxiliary electrode, and an aqueous saturated calomel reference electrode (SCE) were used in the cyclic voltammetry experiments. All electrochemical experiments were performed under a dinitrogen atmosphere. All electrochemical data were collected at 298 K and are uncorrected for junction potentials.

Crystallography. Single crystals of complexes **1**, **2**, and **3** were obtained by slow evaporation of the acetonitrile solutions of the respective complexes. Selected crystal data and data collection parameters are given in Table 4. Data were collected on a Bruker CCD diffractometer using graphite-monochromated Mo K α radi-

ation. X-ray data reduction and structure solution and refinement were done using the SHELXS-97 and SHELXL-97 programs.¹⁰ The structures were solved by the direct methods.

Acknowledgment. Financial assistance received from the Department of Science and Technology (Grant No. SR/S1/IC-15/2004) is gratefully acknowledged.

Note Added after ASAP Publication. The spelling of an author's name was corrected and ref 4a was updated in the version reposted on November 2, 2007.

Supporting Information Available: Mass spectrum of complex **1** (Figure S1), mass spectrum of complex **2** (Figure S2), C–H--- π interactions in complex **2** (Figure S3), mass spectrum of complex **3** (Figure S4), C–H--- π interactions in complex **3** (Figure S5), partial MO diagrams of complex **2** (Figure S6) and complex **3** (Figure S7), and X-ray crystallographic data of complexes **1**, **2**, and **3** in CIF format. This material is available free of charge via the Internet at <http://pubs.acs.org>.

OM700826T

(10) Sheldrick, G. M. *SHELXS-97* and *SHELXL-97*, Fortran programs for crystal structure solution and refinement; University of Göttingen: Göttingen, Germany, 1997.